State of the Art Power-in Tube Niobium-Tin Superconductors

A. Godeke

Lawrence Berkeley National Laboratory, 1 Cyclotron Road, Berkeley CA 94720

A. Den Ouden, A. Nijhuis, H. H. J. ten Kate

Low Temperature Division, Faculty of Science and Technology, University of Twente, P.O. Box 217, 7500 AE, Enschede, The Netherlands

This work was supported by the Director, Office of Science, Office of Basic Energy Sciences, of the U.S. Department of Energy under Contract No. DE-AC02-05CH11231.

State of the Art Powder–in–Tube Niobium–Tin Superconductors

A. Godeke [a,*], A. den Ouden [b], A. Nijhuis [b], H. H. J. ten Kate [b]

[a] *Ernest Orlando Lawrence Berkeley National Laboratory, One Cyclotron Rd., Berkeley, CA 94720, USA*

[b] *Low Temperature Division, Faculty of Science and Technology, University of Twente, P.O. Box 217, 7500 AE, Enschede, The Netherlands*

Abstract

Powder–in–Tube (PIT) processed Niobium–Tin wires are commercially manufactured for nearly three decades and have demonstrated a combination of very high current density (presently up to 2500 Amm^{-2} non-Cu at 12 T and 4.2 K) with fine (35 μm), well separated filaments. We review the developments that have led to the present state of the art PIT Niobium–Tin wires, discuss the wire manufacturing and A15 formation processes, and describe typical superconducting performance in relation to magnetic field and strain. We further highlight successful applications of PIT wires and conclude with an outlook on possibilities for further improvements in the performance of PIT Niobium–Tin wires.

Key words: Powder–in–Tube, Niobium Tin, Nb_3Sn, superconducting wire
PACS: 74.70.Ad, 74.62.Bf, 74.25.Sv

1. Introduction

The construction of superconducting magnets that are able to generate magnetic fields in the 10 to 22 T range requires the use of wires that are based on the A15 phase of intermetallic Niobium–Tin, generally referred to as Nb_3Sn wires. Nb_3Sn superconducting magnets are used in High Energy Physics (HEP), Fusion Energy applications such as the International Thermonuclear Experimental Reactor (ITER), in chemical analysis in Nuclear Magnetic Resonance (NMR) systems, and in standard high field laboratory magnets.

A common requirement is obviously a high critical current density (J_c) but in HEP this is combined with a large adiabatic and dynamic stability. Such stability can be achieved by fine, well separated, twisted filaments with a close proximity of stabilizing high purity Cu. The high ramp-rates in experimental fusion reactors generate significant, undesired, AC losses that can be counteracted by extensive twisting of fine filaments in wires, and by using transposed wires in a cable. Both HEP and fusion typically require an optimized J_c at about 50% of the upper critical magnetic field (H_{c2}), but this optimization is often hindered by the required fine filaments. In NMR, AC losses are less of an issue but a very high H_{c2} is needed to retain sufficient current carrying capacity at very high magnetic fields.

Nb_3Sn wires can be manufactured through various processes. The main commercial processes to date are the Bronze process [1], the Internal–Tin (IT) process [2], and the PIT process. The Bronze process utilizes Nb or Nb–alloy rods that are embedded in a high Sn bronze matrix, which is surrounded by a diffusion barrier and a pure Cu stabilizer. Wire drawing requires intermediate annealing steps after about 50% area reduction, due to the work hardening of the bronze. The Bronze process results in very fine ($\leq$ 5 μm) filamentary wires which can carry relatively low critical current densities as a result of a limited solubility of Sn in the bronze.

In the IT process, a Sn or Sn–alloy core is surrounded by Nb or Nb–alloy rods in a Cu matrix (Rod Restack process or RRP), or by expanded Nb or Nb–alloy mesh which is layered with Cu (Modified Jelly Roll or MJR process). The resulting filament regions (sub-elements) are surrounded by a diffusion barrier and a pure Cu stabilizer. The filaments within a sub-element often grow together during the A15 formation reaction, resulting in an effective filament of the size of a sub-element. IT processed Nb_3Sn wires can carry up to a present record non-Cu current density of about 3000 Amm^{-2} at 12 T and 4.2 K. (All the J_c values in the remainder of this article are quoted at 12 T and 4.2 K, unless mentioned otherwise.) The high current IT wires have been hindered by a relatively large effective filament size (typically $\geq$ 60 μm), but recent restacking attempts have reduced the attainable sub-element sizes in IT wires down to below 50 μm, i.e. approaching PIT level [3,4].

Bronze and IT processed wires thus for long had either a high J_c *or* fine filaments. The PIT process has been, until very recently, the only process available to combine fine filaments *and* a close to record J_c.

* Corresponding author. Phone +1 510 486 4356, Fax +1 510 486 5310
Email address: agodeke@lbl.gov (A. Godeke).

2. History of Powder–in–Tube wires

2.1. *The ECN process*

Manufacture of superconducting wires utilizing a powder in a tube was first proposed by the Netherlands Energy Research Foundation (ECN), Petten, The Netherlands in 1975, and initially referred to as the ECN process. The first PIT processes [5,6] involved filling V tubes with V_2Ga_5 or VSi_2 powders plus 5 to 10% Cu. These tubes were stacked inside a pure Cu matrix, drawn down to final dimension, and reacted to create multifilamentary V_3Ga and V_3Si wires.

The first prototype Nb–Sn PIT wires were manufactured in 1977 [7] from $NbSn_2$ plus 5 to 15% Cu powder in a Nb tube. Multiple tubes were stacked in a pure Cu matrix to yield a 36 filament Nb_3Sn wire. ECN further developed a 180 filament prototype, demonstrated an A15 layer J_c of 2400 Amm^{-2}, and predicted 600 Amm^{-2} overall [8], which was indeed achieved about 5 years later.

In 1981, Elen *et al.* [9] reported on a first production wire, of which about 20 kg was manufactured. This was a 19 filament wire with a diameter of 0.56 mm, which carried 3270 Amm^{-2} in the A15 layer and 248 Amm^{-2} overall. The latter translates, using the reported fractions, to about 475 Amm^{-2} non-Cu. Extrusion was attempted but hindered by Nb tube perforation and the powder specification proved critical for extrusion possibilities.

Production runs of 18 filament wire [10] pointed out the relevance of the powder specifications in relation to the achievable core diameter. Also a 36 filament wire was manufactured by drawing only and a 54 filament, > 90% Cu version was successfully extruded and drawn. Veringa *et al.* [11] then reported an extensive A15 growth kinetics study, and determined a minimum required Cu content in the powder for A15 formation below 700 °C, which was later reported to be 3 wt.% [12].

In 1984 the reported J_c had increased to 500 Amm^{-2} overall and 1140 Amm^{-2} non-Cu [12]. Here, also a first attempt to create ternary A15 was reported through the addition of Ti, Ta, Mg and Ga to the powder core. Ti, Ta, Mg have no apparent effect on the critical properties, presumably since they do not diffuse sufficiently into the A15. With the addition of Ga, the large grain intermediate phase at the core is prevented, but Ga also slows the reaction. A striking agreement is presented between measurements and calculations [13,14] of adiabatic stability as a function of magnetic field and A15 diameter, indicating intrinsic stability in PIT wires for all magnetic fields at A15 diameters below 55 μm.

In 1988, 200 kg of a 36 filament wire was manufactured and a 192 filament wire was at the production stage [15]. Developments towards smaller filament size using restacks resulted in up to 1332 filament prototype wires. Smaller filaments clearly required a shorter reaction time, presumably as a result of smaller diffusion distances. Reported non-Cu current densities for the 36 and 1332 filament wires are 1730 Amm^{-2} and 1650 Amm^{-2} respectively at 11 T, leading (assuming 20% J_c loss per tesla) to a J_c(12 T) of 1384 Amm^{-2} and 1320 Amm^{-2} respectively.

By 1990 [16], the 192 filament wire with 55% Cu appears as a standard product with an average non-Cu J_c(11 T, 4.2 K) of 2120 Amm^{-2} yielding (at −20%/T) J_c(12 T) ≅ 1700 Amm^{-2}. This wire was used to manufacture Rutherford-type cables which were measured at the University of Twente, Enschede, The Netherlands, to carry 19.3 kA at 11 T and 4.2 K, indicating about 10% cabling degradation.

2.2. *Powder–in–Tube wires from ShapeMetal Innovation*

During the first half of the 1990's, ECN discontinued the manufacture of PIT wires. However, the development and manufacture of PIT wires was continued by ShapeMetal Innovation (SMI), Enschede, The Netherlands. SMI focussed on the manufacture of 36 filament wire for very high magnetic field applications and a 192 filament version for HEP magnets. Also development of wires with an increased number of filaments and smaller filament diameter continued at SMI. These developments resulted in the production of a 0.9 mm diameter, 492 filament wire with a filament diameter of about 20 μm and a Cu fraction of 54% [17]. The reported non-Cu current density is 1890 Amm^{-2} at 10 T and 4.2 K, which translates (at −20%/T) to just over 1200 Amm^{-2} at 12 T.

Further optimization of the layout, powder specifications and manufacturing procedures led to a 0.9 mm diameter, 504 filament wire with about 25 μm filaments and a Cu fraction of 52% [18]. This wire carried a non-Cu J_c of 2680 Amm^{-2} at 10 T and 4.2 K, translating to over 1700 Amm^{-2} at 12 T. Also, cold hydrostatic extrusion was successfully employed. For the first time a successful ternary wire was manufactured through the use of a Nb–7.5 wt.% Ta tube in a 37 filament wire with a Cu fraction of 43%. This ternary wire carried about 1750 Amm^{-2}, and 217 Amm^{-2} at 20 T and 4.2 K. This was combined with an increased effective critical field of 25.5 T, compared to an extrapolated 21 T for the binary wires. In the end of the 1990's also new optimized binary and ternary 192 filament wires were manufactured by SMI with reported non-Cu current densities of 1955 Amm^{-2} and 2250 Amm^{-2}, respectively [19]. The latter value translates, using 2380 μm^2 and 935 μm^2 for the non-Cu area and the fine grain A15 area respectively [20], to over 5700 Amm^{-2} in the fine grain A15.

Modern SMI-PIT wires include low AC loss binary and ternary versions of a 504 filament, 0.81 mm wire (Fig. 1, left), with approximately 25 μm filaments, 55% Cu and J_c ≅ 1350 Amm^{-2} and 1950 Amm^{-2} for the binary and ternary versions respectively. Modern high current density conductors include a ternary 288 filament, 1.255 mm wire (Fig. 1, right), with approximately 35 μm filaments, 55% Cu and a J_c = 2500 Amm^{-2} (section 4).

2.3. *Powder–in–Tube wires from Supercon*

The success of the PIT process to combine a very high non-Cu current density with a small filament diameter, the possibility to draw wires without intermediate heat treatments,

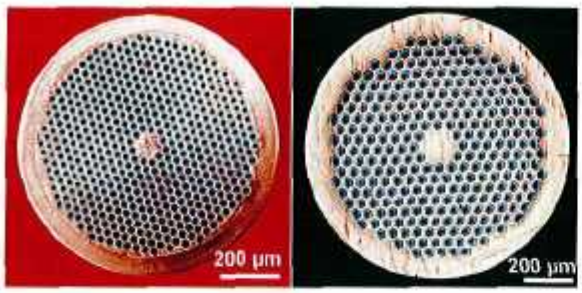

Fig. 1. Modern 504 filament (left) and 288 filament (right) PIT wires, manufactured by SMI.

the short reaction heat treatment, and the clear potential for further optimizations, stimulated Supercon, Shrewsbury MA, USA, to also start PIT manufacture with some novel modifications [21]. Their early process does not use commercial Nb or Nb–7.5 wt.% Ta tubes, but tubes that are fabricated in-house from fine grain Nb, Nb–Ta and Nb–Ti alloy sheet. This creates the possibility to use commercially available alloys (e.g. Nb 7.5 wt.% Ta and Nb 48 wt.% Ti) and adjust the ternary percentages to what is optimal for the superconducting properties, i.e. 1.5 at.% Ti or 3.5 at.% Ta [22]. This is both cost effective and benefits from the homogeneity and fine granularity that come with the commercial large scale manufacture of alloys. In addition, Supercon investigated various methods for cost effective $NbSn_2$ powder manufacture, which are detailed in their publication. A key modification in their process is that the filaments are surrounded by a thin Ta diffusion barrier. This enables a complete transformation of the Nb or Nb-alloy tube to A15, without the risk of poisoning the Cu matrix.

Supercon's initial attempts to fabricate wires were hindered by a too large particle size in the powder. Development of powder manufacturing processes [23] resulted in a successful 18 filament wire with filament diameters below 60 μm and a non-Cu J_c of 1258 Amm^{-2}, and an A15 layer J_c of 4158 Amm^{-2}. Continued development [24] resulted in filaments below 50 μm, an optimized 19 filament binary wire with a non-Cu J_c of 1397 Amm^{-2}, and a prototype 78 filament ternary wire with a non-Cu J_c of 2151 Amm^{-2}. Also hydrostatic extrusion was successfully employed.

Supercon then deviated from the sole use of $NbSn_2$ to alternative cores to provide the Sn and referred to it as the Internal–Tin–Tube process. Similar methods are used at SupraMagnetics, Plantsville CT, USA [25], and the National Institute for Materials Science, Tsukuba, Japan [26]. These new processes will be discussed in section 6. A summary for the achieved current densities in $NbSn_2$ based PIT wires is given in Fig. 2.

3. Wire manufacture and A15 formation

3.1. *Wire manufacture*

The manufacture of PIT wires starts with the production of $NbSn_2$ powder. The details of the powder processes are proprietary but, in general, some free Sn and a minimum of 3 wt.% Cu are added. Cu is known to destabilize the $NbSn_2$ and Nb_6Sn_5

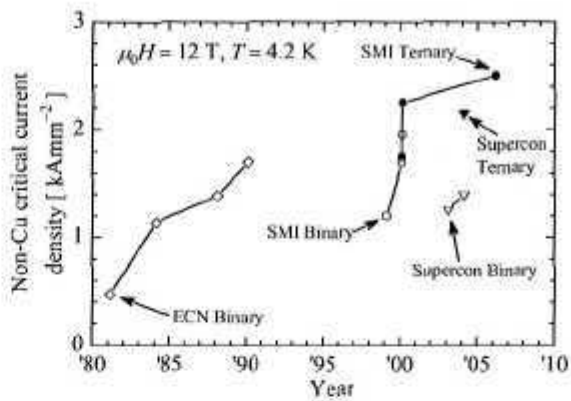

Fig. 2. Non-Cu critical current density as a function of time for binary and ternary $NbSn_2$ powder based PIT processed wires.

line compounds [27] which, combined with the large Sn gradient, enables a rapid A15 phase formation below 700 °C. The powder is placed inside Nb or Nb-alloy tubes, which can be commercially purchased or made from sheet to enable custom compositions. The resulting rods are optionally surrounded by a diffusion barrier and stacked inside a high purity Cu matrix. After an optional extrusion step, which is required for large production lengths, the billet can be cold drawn to final size without the need for intermediate heat treatments. The latter is a key advantage in comparison to the Bronze process.

3.2. *A15 formation reaction*

The A15 phase is formed during a solid state diffusion reaction at a suitable time and temperature combination, which is typically a few days at 675 °C. The Sn diffusion process and A15 formation reaction are visualized in Fig. 3 and extensively described elsewhere [11,20,28]. The Nb-Sn phase diagram [29] dictates that Sn depletion of $NbSn_2$ first results in Nb_6Sn_5, and finally in the A15 phase. The initial Nb_6Sn_5 phase grows inward as well as outward, since the volume per Nb atom in Nb_6Sn_5 is approximately doubled with respect to pure Nb [11]. This intermediate Nb_6Sn_5 phase is indeed detected in the early stage of the reaction [7] and identifiable as the lightest grey area which surrounds the core in the 4 hours at 675 °C cross-section in Fig. 3. After 16 hours, the initial Nb_6Sn_5 phase is no longer visible and transformed into large grain A15 Nb-Sn. The formation of these large A15 grains around the core region is suggested to be a result from the fact that they grow in the presence of a liquid bronze phase [12]. The void fraction in these regions is attributed to the reduced volume of Nb in A15 Nb-Sn, relative to Nb_6Sn_5 [11]. These voids contain a Cu-rich bronze phase since Cu is expelled from the A15, due to the very limited solubility of Cu in the A15 phase.

The A15 is formed outward from the large grain region by a diffusion reaction into the Nb. The A15 formation halts after about 64 h at 675 °C in the example in Fig. 3, due to Sn depletion of the core-A15 interface region [28]. Longer reaction does not result in a further increase of the A15 volume. The

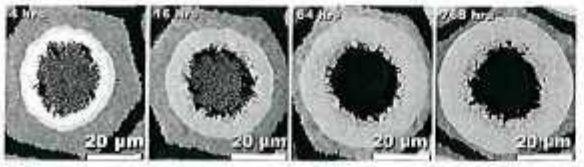

Fig. 3. Reaction progress in the filaments as a function of time at a temperature of 675 °C for a ternary 192 filament PIT wire, manufactured by SMI [19]. Courtesy of C. M. Fischer and P. J. Lee.

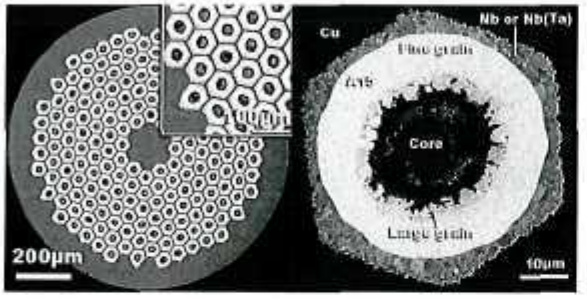

Fig. 4. Ternary 192 filament PIT wire manufactured by SMI, after a heat treatment of 64 h at 675 °C [19,28]. Courtesy of C. M. Fischer and P. J. Lee.

final resulting A15 fraction is of importance to filaments that are not provided with a diffusion barrier. The area fractions have to be properly balanced to prevent poisoning of the high purity Cu matrix, and the resulting decrease in the residual resistive ratio (RRR), which is undesirable for the dynamic stability. Commercial wires without a diffusion barrier are balanced with respect to the reacted Nb and exhibit typical RRR values that are significantly above 100.

3.3. *Exemplary cross-section, morphology and composition*

A typical cross-section after reaction of a 192 filament, ternary PIT wire, which was manufactured by SMI, is presented in Fig. 4. A total cross-section of the wire is presented on the left side in Fig. 4, and the inset shows an enlargement of the filament area. The right side of Fig. 4 shows an enlargement of a typical filament after reaction. The various areas that can be distinguished are fine grain A15 (40%), large grain A15 (10%), unreacted Nb or Nb-alloy (25%), and the core remainder enclosed by the large grain A15 (25%). The percentages reflect fractions of the filament and thus of the non-Cu area. Considering that typically 50% of the wire is non-Cu, and that the large grain A15 does not contribute to superconducting current transport (due to lack of pinning possibilities), typically only 20% of the total wire cross-section carries superconducting current.

That the large grain A15 does not contribute to superconducting current arises from the fact that the maximum pinning force increases significantly with a reduction of the average grain size [22], which leads to the conclusion that the grain boundaries are the main pinning sites in Nb_3Sn. Retaining a small grain size is thus of key importance for the maximum pinning force. In addition, to retain sufficient current carrying capacity towards higher magnetic fields, the grain size should preferably be comparable to the vortex spacing at operational

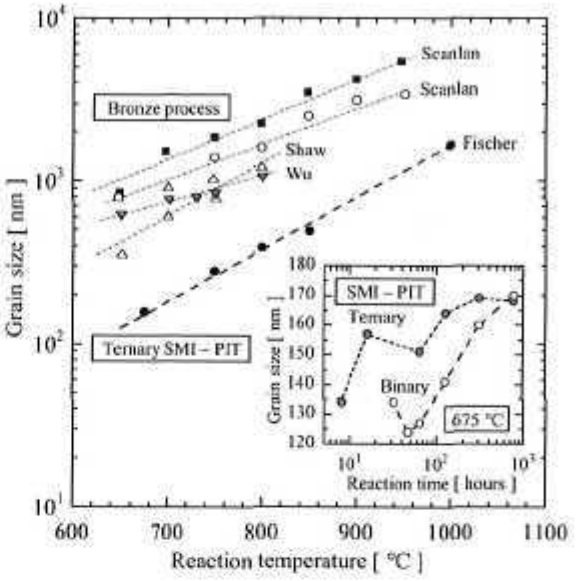

Fig. 5. Average grain size in Nb_3Sn wires as a function of reaction temperature and time (inset) [28]. The PIT results – which only reflect the fine grains – are from Fischer [20], and the Bronze results are from Scanlan *et al.* [33], Shaw [34], and Wu *et al.* [35].

magnetic fields [22,30,31], which is 10 to 20 nm at magnetic fields around 15 T.

The average grain size depends marginally on reaction time and strongly on reaction temperature, as can be seen from Fig. 5, in which also a comparison is made to available Bronze processed wire results. Note that the Bronze results stem from around 1980, and that most modern commercial Bronze processed, IT and PIT wires exhibit grain sizes between 100 and 200 nm at optimal reaction time and temperature. Retaining a small grain size requires balancing of the reaction temperature between the desired small grain size and acceptable reaction times, since a higher reaction temperature will evoke a much faster diffusion reaction [20]. The average grain sizes between 100 to 200 nm for optimized reactions are one order of magnitude above the vortex spacing at application magnetic fields, which results in up to 50% loss in the maximum pinning force [22] and a collective pinning of vortex bundles. The latter causes the maximum pinning force to occur at only 20% of H_{c2} [32] as opposed to 50% of H_{c2} as is achieved in NbTi through the inclusion of $\alpha-$Ti precipitates [30,31]. Further optimization through grain refinement is therefore desirable.

The solid state diffusion of Sn from the core outward into the Nb or Nb-alloy, combined with the fact that the A15 phase is stable from about 18 to 25% Sn, results in a radial compositional gradient. These gradients, and their effect on the superconducting properties have been extensively analyzed [12,19,22,28,36–41] and effectively, these compositional gradients result in gradients in H_{c2} and T_c, leading to effective values (i.e. H_{c2}^* and T_c^*) that determine the critical current density. A typical example of compositional gradients in the A15 phase in PIT wires is presented in Fig. 6. Note that the depicted Sn contents are adjusted by +1.5% to correct for an analysis with uncalibrated EDX [28]. The compositional gradient in PIT wires is about

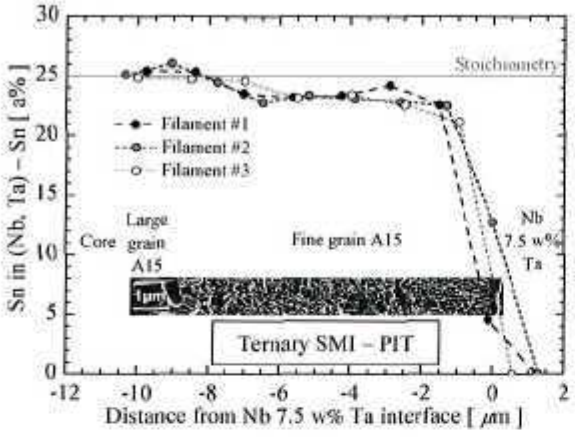

Fig. 6. Atomic Sn content in (Nb,Ta)-Sn as a function of position, measured with Electron Dispersive X-ray Spectroscopy on three filaments in a 192 filament ternary PIT wire, manufactured by SMI and reacted for 64 hours at 675 °C [28]. The inset shows a high resolution fracture micrograph (courtesy of P. J. Lee) of a filament to indicate the approximate position of the measurements.

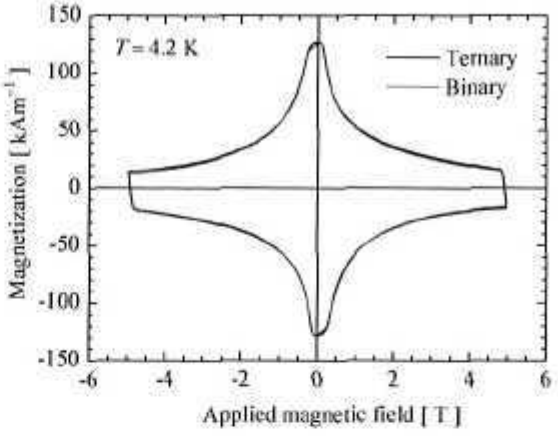

Fig. 7. Magnetization of binary and ternary 504 filament PIT wires, manufactured by SMI, as functions of an applied magnetic field ramp of 5 mT/s.

-0.3 at.% Sn/μm, which is much smaller than in Bronze processed wires (which typically exhibit -4 at.% Sn/μm [42]), but larger than in IT wires. In the latter, inter-filamentary Cu in the sub-elements is believed to enable rapid Sn diffusion, resulting in an all-sided A15 growth into the thin (typically $< 5\mu$m) Nb filaments. The average Sn content across a sub-element in a modern IT wire is about 24 at.% with local variations ranging from about 20 to 26 at.% [43]. Recent analysis by Lee and Larbalestier on record setting IT wires reports 24 ± 1 at.% Sn and an average Sn gradient of only -0.1 at.% Sn/μm [3,44]. This high average Sn content is – amongst others – a major determinant for the achieved 3000 Amm^{-2} [45]. For now, modern PIT wires achieve 2500 Amm^{-2} (see section 4) but compositional and A15 fraction optimization could lead to a significant further increase [19,28,40] (see section 6).

4. Performance in relation to magnetic field and strain

4.1. *Magnetization in relation to transport results*

A key benefit of PIT wires is the possibility to combine large transport current densities with small, well separated filaments, to obtain a wire that is intrinsically stable and, in addition, exhibits low AC losses. Usually, however, an *effective* filament diameter is considered in discussions on stability, since A15 diameters are often not well defined and/or filaments can be not well separated. We will demonstrate below, that for PIT wires the effective and actual diameters are the same, as a result of the nearly perfect cylindrical shaped A15 area inside the Nb tubes, and the perfect filament separation.

A magnetization measurement of a binary and a ternary version of a 0.9 mm diameter, 504 filament PIT wire (Fig. 1) with about 25 μm filaments is shown in Fig. 7. Both wires exhibit virtually indistinguishable magnetization. Also, both wires do not show any flux-jump related instabilities, as would be visual from spikes in the magnetization curve. For completeness, it should be mentioned that flux jumps are observed in PIT wires with filament diameters of 50 μm and larger, as also follows from calculation [13,14]. Nevertheless, these flux jumps generally do not result in low magnetic field instabilities, as a result of the high purity and proximity of the Cu matrix, which apparently provides sufficient dynamic stabilization.

A non-Cu critical current density can be derived from magnetization results as depicted in Fig. 7, if an *average* critical current density is assumed in the A15 tubular volumes. At higher magnetic fields this is physically incorrect, since low Sn A15 would not carry any superconducting current [22]. At magnetic fields below 5 T, however, all A15 can be expected to be superconducting. For a PIT conductor, with its tubular A15 volume inside the filaments, the magnetic moment m of a sample with a length l can be described by:

$$m = \frac{1}{6} J_{c,A15} d_{A15,o}^3 n l \left(1 - \left(\frac{d_{A15,i}}{d_{A15,o}}\right)^3\right), \qquad (1)$$

where $J_{c,A15}$ represents the average critical current density in the A15, $n = 504$ is the number of filaments, and $d_{A15,i} = 10\ \mu$m and $d_{A15,o} = 22\ \mu$m are the inner and outer A15 diameters, respectively (large grains included). Resulting $J_{c,A15}$ values, derived from magnetization measurements and averaged over increasing and decreasing magnetic field for two samples, are graphed in a usual Kramer plot with $p = 0.5$ and $q = 2$ [32] in Fig. 8 for ternary and binary versions of a 504 filament wire. Included in Fig. 8 are self-field corrected transport critical current results at higher magnetic fields on the same wires, and a Kramer extrapolation of the higher magnetic field transport results to lower magnetic field.

The Kramer extrapolation is able to predict the magnetization results strikingly well, aside from the small deviations between 2 and 4 T. This leads to two conclusions: 1) Kramer plots, using $p = 0.5$ and $q = 2$, are linear down to below 1 T, in agreement with earlier conclusions [32]. 2) The tubular A15 volume is a reasonable estimate for the superconducting volume and, hence, its outer diameter is the actual, as well as the effective filament diameter. Note that the Kramer plots for the binary and

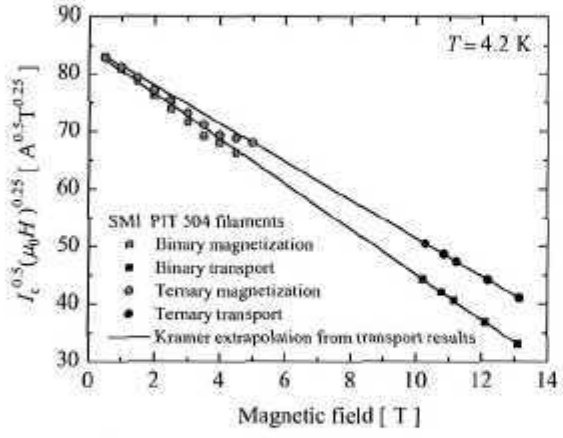

Fig. 8. A Kramer plot of transport critical current as a function of self-field corrected magnetic field, compared to critical current data that is calculated from magnetization measurements. The line represents a Kramer extrapolation of the transport critical current results to low magnetic field.

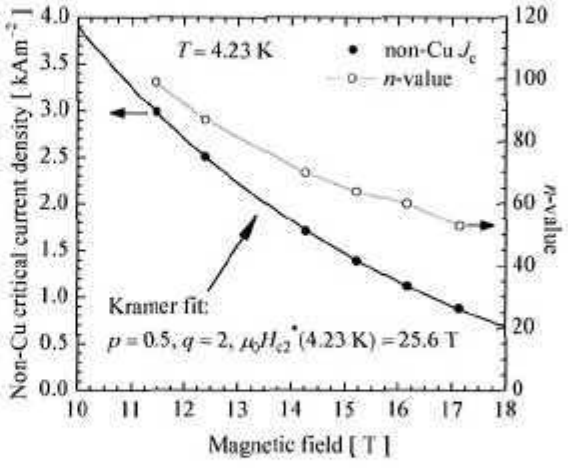

Fig. 9. Non-Cu critical current density and n-value as functions of self-field corrected magnetic field.

ternary wires extrapolate to identical values when $H \to 0$. This implicates, since $I_c^{0.5}(\mu_0 H)^{0.25}_{H\to 0} = cH_{c2}/\kappa_1 = cH_c$ [32], where κ_1 represents the Ginzburg-Landau parameter, H_c is the thermodynamic critical magnetic field, and c is a constant related to the maximum pinning force, that the product cH_c is comparable for both wires.

4.2. *Critical current density and n-value as a function of magnetic field*

The present record current density PIT wire, developed for the Next European Dipole Joint Research Activity [46], is a ternary 288 filament wire as shown in Fig. 1. The critical current density and n-value as functions of magnetic field are depicted in Fig. 9. In this graph, the applied magnetic field is corrected for the self-field on the filamentary area in the wire ($\varnothing \cong 1.046$ mm), resulting in a self-field correction of 0.284 T/kA [28]. Included in the plot is a fit on the J_c results using common scaling relations [32], indicating $\mu_0 H_{c2}^*(4.23\ \mathrm{K}) =$ 25.6 T, which is typical for ternary PIT.

The n-value for this wire is above 50 at 17 T. The n-value in low temperature superconductors is determined intrinsically through thermally activated flux-flow when approaching J_c but, due to the low temperature, dominated by inhomogeneities [28]. The n-value is generally high (> 60 at 12 T) for most PIT wires, presumably mainly as a result of the compositional and geometrical homogeneity of the A15. This renders PIT wires highly suitable for applications that require a high n-value, such as NMR.

4.3. *Strain sensitivity*

PIT wires exhibit, like other processed wires, a sensitivity to strain, as a result of the intrinsic strain sensitivity of Nb_3Sn [22]. A key difference between PIT wires and other processes is that the axial thermal pre-compression can be lower than in other wires, presumably due to yield in the pure Cu matrix during cooldown. As a result of this lower pre-compression, PIT wires could enter the tensile strain region sooner. The irreversible strain limit, which can be correlated to the formation of cracks in the A15, could therefore be reached earlier, when PIT wires are loaded with tensile forces. Magnet designs have to be optimized to account for this possibility of a lower axial pre-compression.

Veringa *et al.* [11] reported the first strain dependence characterizations on PIT wires, which suggest crack formation above 0.3% bending strain. In 1990, the irreversible strain limit which results from crack formation in the A15 was related to filament diameter [16]. Measurements showed an irreversible axial strain limit of 0.2% for 60 μm filaments and 0.6% for 30 μm filaments. Crack formation at 0.6% tensile strain agrees with recent bending tests that have been performed on more modern PIT wires with 50 μm filaments. In that research, cracks start to appear in PIT at 0.6% tensile strains, and this outperformed Bronze and IT wires in the same research [47].

The axial strain sensitivity of PIT processed wires is generic and not significantly different from wires that are manufactured through other processes, even though the normalized strain sensitivity of J_c can appear somewhat increased in comparison to relatively lower current density Bronze and IT processed conductors [48,49]. Origins of this observable difference in strain sensitivity at 12 T are a different Sn content in the A15 and the presence or absence of ternary additions, which both lead to differences in the long range ordering and the effective H_{c2}.

Strain in A15 Nb-Sn affects the electron-phonon interaction and the density of states, and therefore causes a shift in $H_{c2}(T)$ [22]. It can further be argued that strain will not significantly change pinning efficiency, and strain dependence is therefore usually described as the ratio between the strain modified field-temperature phase boundary ($H_{c2}(T,\varepsilon)$), and the maximum field-temperature phase boundary for which the strain is minimized ($H_{c2\max}(T)$) [32]. The nett effect of a higher $H_{c2\max}(T)$ (i.e. a higher effective upper critical field H_{c2}^* in a wire) on the strain dependence of J_c at a given magnetic field follows through common scaling relations for the critical cur-

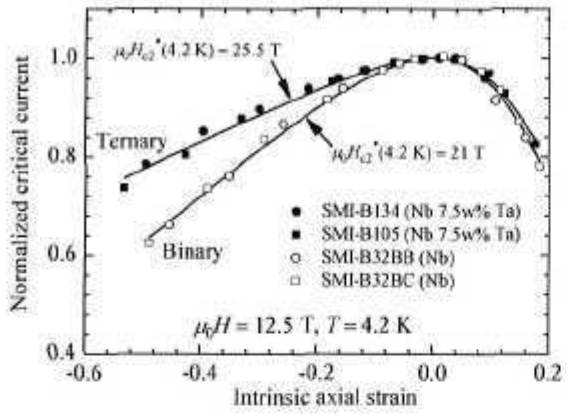

Fig. 10. Normalized critical current as a function of intrinsic axial strain for four different wires from three different billets. Billets B134 and B105 were made using Nb 7.5 wt.% Ta tubes and billet B32 is made using pure Nb tubes. The lines are fits from scaling relations [32], using parameters as depicted in Table 1.

rent density [32]: Increasing H_{c2}^* results in a smaller relative reduction of J_c with strain at a given magnetic field. H_{c2}^* should therefore be reflected in strain sensitivity comparisons, but this is often not included.

Both the Bronze and IT wires in the comparisons in [48,49] are ternary, whereas the investigated PIT wire is binary. In Fig. 10, a comparison is shown between wires from three different billets. Two of the wires are ternary and two are binary. It is evident from this comparison that the ternary wires exhibit a significantly reduced strain sensitivity at 12.5 T. The introduction of Ta in the A15 lattice reduces the long range ordering in the A15 lattice. It was suggested elsewhere [22] that this alone can result in a reduced strain sensitivity. Also, a key effect of adding ternary additions is that the A15 lattice is stabilized for compositions above 24.5 at.% Sn, thereby preventing the occurrence of the tetragonal lattice distortion and the accompanying lower H_{c2}. In addition, it is generally stated that the introduction of Ta increases scattering, and thus the normal state resistivity and H_{c2}.

Typical values for $\mu_0 H_{c2}^*(4.2\ \mathrm{K})$ for ternary and binary SMI-PIT wires are 25.5 T and 21 T respectively [18]. The normalized $J_c(12.5\ \mathrm{T},\ 4.2\ \mathrm{K},\ \varepsilon_a)$ results in Fig. 10 were least squares fitted using scaling relations [32] for both the binary (B32) wires and for one ternary wire (B105), using the parameters in Table 1. The lines in Fig. 10 reflect these parameterizations. The maximum zero temperature, effective upper critical field values ($H_{c2max}^*(0)$) that were used in the fits result in $\mu_0 H_{c2}^*(4.2\ K, -0.2\%) = 25.5$ T and 21 T for the ternary and binary wires respectively, assuming an intrinsic axial thermal pre-compression of -0.2%.

The increased strain sensitivity for the binary wires can be mainly attributed to a lower effective upper critical magnetic field. This can be demonstrated by calculating a least squares fit to the ternary and binary data with *identical* deformation parameters and varying *only* $H_{c2max}^*(0)$. Such a fit shows that the calculated shift in $J_c(\varepsilon)$ by varying only $H_{c2max}^*(0)$ is of the correct magnitude. Accurate fits to the data, however, cannot

Table 1
Scaling parameters for the lines in Fig. 10. The applied scaling relations and parameters are detailed in [32].

	Deformation			Superconducting	
	C_{a1}	C_{a2}	$\varepsilon_{0,a}$	$\mu_0 H_{c2max}^*(0)$	$T_{cmax}^*(0)$
Billet			[%]	[T]	[K]
B105	58.1	36.3	0.117	29.3	17
B32	64.1	36.1	0.165	24.2	17

be achieved by only a different $H_{c2max}^*(0)$, and require also a slight difference in the deformation parameters (Table 1). It is very reasonable, and physically more correct, to expect differences in the deformation parameters for wires from different billets with dissimilar layout. Nonetheless, the main difference between the ternary and binary wires can be attributed to a different $H_{c2max}^*(0)$, indicating that the normalized strain dependence of $H_{c2}^*(0)$ is comparable for both wires, and emphasizing the need to consider the magnitude of H_{c2}^* in strain sensitivity comparisons.

For completeness, it should be mentioned that also differences in Sn content could attribute to differences in strain sensitivity. There are strong indications that Sn richer A15, which is closer to stoichiometry and thus has a higher degree of ordering in the A15 lattice, has an increased strain sensitivity, as was suggested elsewhere [22]. Increasing the Sn content in the A15, however, also increases the effective upper critical magnetic field [19] which would reduce the strain sensitivity at constant magnetic field as was shown above. It is, for now, unclear how these opposing effects will average out. It should finally be noted that the result in Fig. 10 is contrary to older work, in which an *increased* strain sensitivity for alloyed wires was observed [50].

Measurements on the sensitivity to transverse pressure in Rutherford-type cables have indicated that PIT behaves better than IT and Bronze processed wires [51]. It should be emphasized, however, that much of the sensitivity to transverse pressure is related to the amount of deformation at the cable edges. This is specifically the case for 'keystoned' cables, where the thin edge is often heavily deformed during cabling. The PIT cable in [51], which behaved favorable, was the only rectangular cable in that comparison. A keystoned PIT cable did indicate severe sensitivity to transverse pressure, even though this was attributed to experimental imperfections. A later keystoned PIT cable exhibited much more favorable transverse pressure sensitivity and this cable was used in the world record setting 11 T dipole magnet developed at the University of Twente, The Netherlands (MSUT) [52–54]. Later experiments on IT cables also indicated a much reduced sensitivity to transverse pressure [55] and Lawrence Berkeley National Laboratory's D20 magnet, in which this cable was used, did achieve a new record dipole magnetic field [56].

From more recent experiments on the transverse pressure sensitivity cables, using a simplified experiment in which one strand is regarded representative for the behavior of a cable, it is concluded that PIT strands exhibit significantly higher pressure sensitivity than MJR and IT wires [57]. Nevertheless, mag-

nets that were made from PIT cables are claimed to reach an 'adjusted' short sample and surpass the performance of IT and MJR based magnets [58–60]. In observing the transverse pressure results, it should be noted that the PIT results are inconsistent, with some strands behaving comparable to MJR and IT samples, whereas others exhibit a more severe reduction of the critical current with pressure. Similar severe reductions have been observed in the past on keystoned cables, made from IT and PIT strands, for which too severe compaction of the cable width was suggested as an origin of increased pressure sensitivity. The PIT cables in [57] were manufactured at a width of 14.24 ± 0.025 mm, which appears small for a 28 strand cable with 1 mm wires, suggesting severe edge deformation. It is reasonable to assume that PIT wires, with solid Nb tubular filaments, are more sensitive to such edge deformation during cabling than the IT wires, which have a significant amount of Cu in the subelements.

Considering the above discussion, it should be stated that, in general, published transverse pressure experiments are ambiguous, and the results depend on experimental and cabling details. Nevertheless, it can be concluded that Rutherford cables, fabricated from PIT wires, appear to experience a similar sensitivity to transverse pressure in comparison to cables made from wires that are manufactured by other methods from the simple fact that magnets, constructed from PIT wires, have performed up to world record magnetic fields with their accompanying loads, provided that the cable is manufactured properly.

5. Successful applications using PIT wires

Powder-in-Tube processed Nb_3Sn wires have been applied successfully in a number of applications. The first application was an 11 T solenoid insert magnet from Oxford Instruments in 1983, which used about 500 m of an 18 filament wire [10]. In 1988, 200 kg 36 filament wire was manufactured for a 12 T insert for the Sultan facility in Villigen, Switzerland [15,61]. Rutherford-type cables were manufactured from 192 filament wire in 1990 and used in the world record setting 11 T MSUT dipole magnet [52–54], which was the first Nb_3Sn dipole to surpass NbTi dipole limitations.

Dipole magnets at Fermi National Laboratory used SMI-PIT wire to overcome the low magnetic field instabilities that are related to the use of large filamentary IT wire [58–60,62]. These magnets achieved a 10 T dipole magnetic field, were claimed to achieve their short sample limitation, and surpassed the performance of earlier magnets at Fermi National Laboratory which employed IT wires.

Further applications include various standard high field magnets, and cryocooler and conduction cooled magnets that operate at temperatures from 8 to 12 K.

These successful applications illustrate the feasibility of PIT processed Nb_3Sn superconductors for solenoidal and HEP magnets. In addition, PIT wires have been successfully developed by SMI for the International Thermonuclear Experimental Reactor.

6. Progress in R&D and outlook to the future

Further possible optimizations of the PIT process can be separated into three groups: 1) Increasing the A15 fraction in the non-Cu area, 2) Increasing the Sn content in the A15, and 3) Increasing the maximum pinning force and high field pinning efficiency.

Optimization of the A15 fraction can be achieved by increasing the Nb or Nb-alloy fraction at the manufacturing stage, by surrounding the filaments with a diffusion barrier [24], and by preventing the formation of large grain A15 [12]. The latter two optimizations have the – theoretical – potential to increase the non-Cu current density by about 65% [28,63]. It should be emphasized that this number represents an idealized situation. In reality, since PIT wire manufacture is a difficult process that depends on many parameters, it is unreasonable to expect that this improvement can be achieved fully in wires.

The Sn content in the A15 volume can – possibly – be increased by allowing more Sn to be available for the reaction. If all fine grain A15 would be approaching stoichiometry then theoretically an increase of about 35% in the non-Cu current density could be expected [28,63]. A combination of A15 fraction and Sn content optimization would thus yield a theoretical 100% increase in the non-Cu current density, or the possibility to approach 5000 Amm^{-2} non-Cu [28]. Although this clearly demonstrates a huge potential, it should again be emphasized that it is unrealistic to expect this to be achieved in wires. For example, simply adding more Sn to the core could significantly hinder wire drawing and, for now, it is unclear whether additional Sn can indeed be evoked to diffuse into the Nb or Nb-alloy without a resulting gradient.

A promising new development is to investigate alternative Sn-rich intermetallics with a higher atomic Sn density that could, in powder form, act as the Sn source in the core [64]. Also, ceramic reinforced pure Sn and Cu-Sn alloys are under investigation as core material. In [65] and [66] a pure Sn, and a pure Sn plus 10 v% Al_2O_3 powder is successfully tried as a Sn source. Also various Cu-Sn alloys (Sn–3 wt.% Cu and Sn–7.6 wt.% Cu) have been tested. Wires made with a pure Sn core reached a J_c of 1251 Amm^{-2} and wires with a Sn–3 wt.% Cu core achieved 1372 Amm^{-2}. It should be noted that such developments will lead to a three step heat treatment, to prevent formation of an undesired Nb–Cu–Sn compound [66,67]. A new process at SupraMagnetics uses Cu_5Sn_4 cores in Nb 7.5 wt.% Ta tubes that were processed down to about 20 μm. These wires achieve a non-Cu J_c of about 2000 Amm^{-2} [25] and are targeted to significantly reduce the cost for PIT processed wires.

The maximum pinning force and high field pinning capacity can be improved by grain refinement and by the introduction of engineered pinning centers in the A15 volume. The potential benefits of matching the spacing of the pinning sites to the vortex spacing can be estimated to be a 50% increase in the maximum pinning force [22], combined with an approximate 40% increase in pinning efficiency at 50% of H_{c2}^* (i.e. around 15 T) [19,31,32]. An additional benefit of grain refinement is

that it will increase scattering and thus the normal state resistivity, which in turn has the potential to further enhance H_{c2} if the mean free path is not too severely reduced [68,69].

7. Conclusions

The Powder-in-Tube Nb_3Sn wire process has proven to yield a combination of high current density with fine filaments. The present record wires achieve a non-Cu current density of 2500 Amm^{-2}, and combine this with a filament diameter of about 35 μm. Wires that are optimized for low AC loss achieve a non-Cu current density of 1950 Amm^{-2} and combine this with a filament size of about 25 μm. The typical high n-value and high RRR make PIT wires suitable for a multitude of applications, which has been demonstrated specifically in successful dipole magnets for High Energy Physics. Further increase in the critical current density as well as a reduction of the manufacturing costs appear very realistic through optimizations of the process parameters and the use of alternative powders. A theoretical limit on achievable current densities can be calculated, but it remains speculative to what extend improvements can be achieved in a large scale manufacturing process. Nevertheless, during the past 15 years, the Powder–in–Tube process has been developed such, that excellent wires can be manufactured on a commercial basis. These wires feature high current density paired to small filaments, properties which are beneficial for most applications, and sometimes even essential for success.

Acknowledgment

The microstructural and microchemistry analysis presented in this publication summarize results that were obtained at the Applied Superconductivity Center in Madison, WI, USA (now at the National High Magnetic Field Laboratory, Tallahassee, FL, USA). This work was supported by the Director, Office of Science, High Energy Physics, U.S. Department of Energy under contract No. DE-AC02-05CH11231.

References

[1] A. R. Kaufmann, J. J. Pickett, Multifilament Nb_3Sn superconducting wire, Bul. Am. Phys. Soc. 15 (6) (1970) 838.

[2] Y. Hashimoto, K. Yoshizaki, M. Tanaka, Processing and properties of superconducting Nb_3Sn filamentary wires, in: Proc. 5th Int. Cryo. Eng. Conf., Kyoto, Japan, 1974, IPC Sci. and Technol. Press, Surrey, England, 1974, p. 332.

[3] P. J. Lee, D. C. Larbalestier, Microstructural factors important for the development of high critical current density Nb_3Sn strand, *ibid.*

[4] D. R. Dietderich, A. Godeke, Nb_3Sn at the frontier. Last achievements in the U.S. strands & cables, *ibid.*

[5] C. A. M. van Beijnen, J. D. Elen, Potential fabrication method of superconducting multifilament wires of the A-15-type, IEEE Trans. Magn. MAG-11 (2) (1975) 243.

[6] J. D. Elen, C. A. M. van Beynen, Critical properties of V_3Ga multifilament wire, Proc. 5th Int. Conf. on Magnet Techn. (MT-5), Roma, Italy (1975) 730.

[7] J. D. Elen, C. A. M. van Beijnen, C. A. M. van der Klein, Multifilament V_3Ga and Nb_3Sn superconductors produced by the ECN-technique, IEEE Trans. Magn. MAG-13 (1) (1977) 470.

[8] C. A. M. van Beijnen, J. D. Elen, Multifilament Nb_3Sn superconductors produced by the E.C.N. technique, IEEE Trans. Magn. MAG-15 (1) (1979) 87.

[9] J. D. Elen, J. W. Schinkel, A. C. A. van Wees, C. A. M. van Beijnen, E. M. Hornsveld, Development of stabilized Nb_3Sn wire containing a reduced number of filaments, IEEE Trans. Magn. MAG-17 (1) (1981) 1002.

[10] A. C. A. van Wees, P. Hoogendam, H. Veringa, Development of high current Nb_3Sn multifilament superconducting material following the ECN powder method, IEEE Trans. Magn. MAG-19 (3) (1983) 556.

[11] H. Veringa, P. Hoogendam, A. C. A. van Wees, Growth kinetics and characterization of superconducting properties of multifilament materials made by the ECN powder method, IEEE Trans. Magn. MAG-19 (3) (1983) 773.

[12] H. Veringa, E. M. Hornsveld, P. Hoogendam, Optimization of high current density A-15 superconductors made by the ECN powder method, Adv. Cryo. Eng. (Materials) 30 (1984) 813.

[13] H. J. Veringa, Electromagnetic instabilities in technical NbTi and Nb_3Sn superconductors, in: Proc. 8th Int. Cryo. Eng. Conf., Genova, Italy, 1980, IPC Sci. and Technol. Press, Surrey, England, 1980, p. 499.

[14] H. J. Veringa, Intrinsic stability of technical superconductors, Ph.D. thesis, University of Twente, The Netherlands (1981).

[15] E. M. Hornsveld, J. D. Elen, C. A. M. van Beijnen, P. Hoogendam, Development of ECN-type Niobium-Tin wire towards smaller filament size, Adv. Cryo. Eng. (Materials) 34 (1988) 493.

[16] E. M. Hornsveld, J. D. Elen, Development of Niobium-Tin conductors at ECN, Adv. Cryo. Eng. (Materials) 36A (1990) 157.

[17] J. H. Lindenhovius, E. M. Hornsveld, A. den Ouden, W. A. J. Wessel, H. H. J. ten Kate, Progress in the development of Nb_3Sn conductors based on the "Powder in Tube" method with finer filaments, IEEE Trans. Appl. Supercond. 9 (2) (1999) 1451.

[18] J. L. H. Lindenhovius, E. M. Hornsveld, A. den Ouden, W. A. J. Wessel, H. H. J. ten Kate, Powder-in-Tube (PIT) Nb_3Sn conductors for high-field magnets, IEEE Trans. Appl. Supercond. 10 (2000) 975.

[19] A. Godeke, M. C. Jewell, C. M. Fischer, A. A. Squitieri, P. J. Lee, D. C. Larbalestier, The upper critical field of filamentary Nb_3Sn conductors, J. Appl. Phys. 97 (2005) 093909.

[20] C. M. Fischer, Investigation of the relationships between superconducting properties and Nb_3Sn reaction conditions in Powder-in-Tube Nb_3Sn conductors, Master's thesis, Univ. of Wisconsin-Madison (2002).

[21] T. Wong, C. V. Renaud, Ti and Ta additions to Nb_3Sn by the Powder in Tube process, IEEE Trans. Appl. Supercond. 11 (1) (2001) 3584.

[22] A. Godeke, A review of the properties of Nb_3Sn and their variation with A15 composition, morphology and strain state, Supercond. Sci. and Techn. 19 (8) (2006) R68.

[23] C. V. Renaud Jr., L. R. Motowidlo, T. Wong, Status of Powder-in-Tube Nb_3Sn conductor development at Supercon, IEEE Trans. Appl. Supercond. 13 (2) (2003) 3490.

[24] C. V. Renaud, L. R. Motowidlo, T. Wong, Nb_3Sn Powder-in-Tube superconductor: Processing, design optimization and properties, Adv. Cryo. Eng. (Materials) 50B (2004) 376.

[25] L. R. Motowidlo, A new PIT Nb_3Sn conductor for high magnetic field applications, Presentation 1MJ07 at the 2006 Applied Superconductivity Conference, Seattle WA, USA (2006).

[26] A. Kikuchi, Y. Yoshida, T. Takeuchi, M. Tomonaga, H. Taniguchi, Y. Monjyu, T. Mizuta, H. Y., K. Tagawa, Development of new PIT-Nb_3Sn multifilamentary wires through the FEAT process, Presentation 1MJ05 at the 2006 Applied Superconductivity Conference, Seattle WA, USA (2006).

[27] G. Lefranc, A. Müller, Effect of copper additions to superconducting niobium-tin sinter material, J. Less Common Metals 45 (1976) 339.

[28] A. Godeke, Performance boundaries in Nb_3Sn superconductors, Ph.D. thesis, Univ. of Twente, Enschede, The Netherlands (2005).

[29] J. P. Charlesworth, I. MacPhail, P. E. Madsen, Experimental work on the Niobium-Tin constitution diagram and related studies, J. Mater. Sci. 5 (1970) 580.

[30] P. J. Lee, D. C. Larbalestier, Niobium-Titanium superconducting wires: Nanostructures by extrusion and wire drawing, Wire Journal International 36 (2) (2003) 61.

[31] A. Godeke, D. Cheng, D. R. Dietderich, P. Ferracin, S. O. Prestemon, G. Sabbi, R. M. Scanlan, Limits of NbTi and Nb_3Sn, and development of W&R Bi-2212 high field accelerator magnets, IEEE Trans. Appl. Supercond. 17 (2) (2007) 1149.

[32] A. Godeke, B. ten Haken, H. H. J. ten Kate, D. C. Larbalestier, A general scaling relation for the critical current density in Nb_3Sn wires, Supercond. Sci. and Techn. 19 (2006) R100.

[33] R. M. Scanlan, W. A. Fietz, E. F. Koch, Flux pinning centers in superconducting Nb_3Sn, J. Appl. Phys. 46 (1975) 2244.

[34] B. J. Shaw, Grain size and film thickness of Nb_3Sn formed by solid state diffusion in the range 650-800°C, J. Appl. Phys. 47 (1976) 2143.

[35] I. W. Wu, D. R. Dietderich, J. T. Holthuis, M. Hong, W. V. Hassenzahl, J. W. Morris Jr., The microstructure and critical current characteristic of a bronze-processed multifilamentary Nb_3Sn superconducting wire, J. Appl. Phys. 54 (12) (1983) 7139.

[36] C. D. Hawes, P. J. Lee, D. C. Larbalestier, Measurement of the critical temperature transition and composition gradient in Powder-in-Tube Nb_3Sn composite wire, IEEE Trans. Appl. Supercond. 10 (1) (2000) 988.

[37] C. D. Hawes, Investigations of the inhomogeneity of a Powder-in-Tube Nb_3Sn conductor, Master's thesis, Univ. of Wisconsin-Madison (2002).

[38] C. D. Hawes, P. J. Lee, D. C. Larbalestier, Measurements of the microstructural, microchemical and transition temperature gradients of A15 layers in a high-performance Nb_3Sn powder-in-tube superconducting strand, Supercond. Sci. and Techn. 19 (2006) S27.

[39] M. C. Jewell, A. Godeke, P. J. Lee, D. C. Larbalestier, The upper critical field of stoichiometric and off-stoichiometric bulk, binary Nb_3Sn, Adv. Cryo. Eng. (Materials) 50B (2004) 474.

[40] L. D. Cooley, C. M. Fischer, P. J. Lee, D. C. Larbalestier, Simulations of the effects of tin composition gradients on the superconducting properties of Nb_3Sn conductors, J. Appl. Phys. 96 (4) (2004) 2122.

[41] A. Godeke, M. C. Jewell, A. A. Golubov, B. ten Haken, D. C. Larbalestier, Inconsistencies between extrapolated and actual critical fields in Nb_3Sn wires as demonstrated by direct measurements of H_{c2}, H^* and T_c, Supercond. Sci. and Techn. 16 (2003) 1019.

[42] V. Abächerli, D. Uglietti, P. Lezza, B. Seeber, R. Flükiger, M. Cantoni, P. A. Buffat, The influence of Ti doping methods on the high field performance of $(Nb,Ta,Ti)_3Sn$ multifilamentary wires using Osprey Bronze, IEEE Trans. Appl. Supercond. 15 (2005) 3482.

[43] D. Uglietti, V. Abächerli, M. Cantoni, A. Reginelli, P. Buffat, H. J. Mathieu, R. Flükiger, Composition, grain morphology and transport properties of Nb_3Sn Bronze Route and Internal Sn wires, Presentation THA01PO06 at the 19th International Conference on Magnet Technology, Genova, Italy (2005).

[44] P. J. Lee, D. C. Larbalestier, Microstructure, microchemistry and the development of very high Nb_3Sn layer critical current density, IEEE Trans. Appl. Supercond. 15 (2) (2005) 3474.

[45] J. A. Parrell, M. B. Field, Y. Zhang, S. Hong, Nb_3Sn conductor development for Fusion and particle accelerator applications, Adv. Cryo. Eng. (Materials) 50B (2004) 369.

[46] A. Devred, B. Baudouy, D. E. Baynham, T. Boutboul, S. Canfer, M. Chorowski, P. Fabbricatore, S. Farinon, H. Felice, P. Fessia, J. Fydrych, V. Granata, M. Greco, J. Greenhalgh, D. Leroy, P. Loverige, M. Matkowski, G. Michalski, F. Michel, L. R. Oberli, A. den Ouden, D. Pedrini, S. Pietrowicz, J. Polinski, V. Previtali, L. Quettier, D. Richter, J. M. Rifflet, J. Rochford, F. Rondeaux, S. Sanz, C. Scheuerlein, N. Schwerg, S. Sgobba, M. Sorbi, F. Toral-Fernandez, R. van Weelderen, P. Vedrine, G. Volpini, Overview and status of the Next European Dipole Joint Research Activity, Supercond. Sci. and Techn. 19 (2006) S67.

[47] M. C. Jewell, P. J. Lee, D. C. Larbalestier, The influence of Nb_3Sn strand geometry on filament breakage under bend strain as revealed by metallography, Supercond. Sci. and Techn. 16 (2003) 1005.

[48] A. Godeke, M. Dhalle, A. Morelli, L. Stobbelaar, H. van Weeren, H. J. N. van Eck, W. Abbas, A. Nijhuis, A. den Ouden, B. ten Haken, A device to investigate the axial strain dependence of the critical current density in superconductors, Rev. Sci. Instrum. 75 (12) (2004) 5112.

[49] A. Nijhuis, Y. Ilyin, W. A. J. Wessel, W. Abbas, Critical current and strand stiffness of three types of Nb_3Sn strand subjected to spatial periodic bending, Supercond. Sci. and Techn. 19 (2006) 1136.

[50] J. W. Ekin, High-field flux pinning and the strain scaling law, in: T. Matsushita, K. Yamafuji, F. Irie (Eds.), Proc. Int. Symp. on Flux Pinning and Electromagnetic Properties in Superconductors, Matsukuma Press, Fukuoka, 1985, p. 267.

[51] H. H. J. ten Kate, H. W. Weijers, J. M. van Oort, Critical current degradation in Nb_3Sn cables under transverse pressure, IEEE Trans. Appl. Supercond. 3 (1) (1993) 1334.

[52] A. den Ouden, S. Wessel, E. Krooshoop, R. Dubbeldam, H. H. J. ten Kate, An experimental 11.5 T Nb_3Sn LHC type of dipole magnet, IEEE Trans. Magn. 30 (4) (1994) 2320.

[53] A. den Ouden, W. A. J. Wessel, H. H. J. ten Kate, Application of Nb_3Sn superconductors in accelerator magnets, IEEE Trans. Appl. Supercond. 7 (2) (1997) 733.

[54] A. den Ouden, H. H. J. ten Kate, A. Siemko, P. Sievers, L. Walckiers, Quench characteristics of the 11 T Nb_3Sn model dipole magnet MSUT, in: L. Liangzhen, S. Guoliao, Y. Luguang (Eds.), Proceedings of the 15th International Conference on Magnet Technology, Science Press, Beijing, China, 1998, p. 339.

[55] D. R. Dietderich, R. M. Scanlan, R. P. Walsh, J. R. Miller, Critical current of superconducting Rutherford cable in high magnetic fields with transverse pressure, IEEE Trans. Appl. Supercond. 9 (2) (1999) 122.

[56] R. M. Scanlan, R. J. Benjegerdes, P. A. Bish, S. Caspi, K. Chow, D. Dell'Orco, D. R. Diederich, M. A. Green, R. Hannaford, W. Harnden, H. C. Higley, A. F. Lietzke, A. D. McInturff, L. Morrison, M. E. Morrison, C. E. Taylor, J. M. van Oort, Preliminary test results of a 13 Tesla niobium tin dipole, in: Applied Superconductivity 1997. Proceedings of EUCAS 1997 Third European Conference on Applied Superconductivity, Vol. 2, Institute of Physics Publishing, Bristol, UK, 1997, p. 1503.

[57] E. Barzi, T. Wokas, A. V. Zlobin, Sensitivity of Nb_3Sn Rutherford-type cables to transverse pressure, IEEE Trans. Appl. Supercond. 15 (2) (2005) 1541.

[58] S. Feher, G. Ambrosio, N. Andreev, E. Barzi, B. Bordini, B. R., R. Carcagno, V. I. Kashikhin, V. V. Kashikhin, M. J. Lamm, I. Novitski, D. Orris, Y. Pischalnikov, C. Sylvester, M. Tartaglia, R. Yamada, A. V. Zlobin, Cable testing for Fermilab's high field magnets using small racetrack coils, IEEE Trans. Appl. Supercond. 15 (2) (2005) 1550.

[59] A. V. Zlobin, G. Ambrosio, N. Andreev, E. Barzi, R. Bossert, R. Carcagno, D. R. Chichili, L. Elementi, S. Feher, V. S. Kashikhin, V. V. Kashikhin, M. J. Lamm, I. Novitski, Y. Pischalnikov, C. Sylvester, M. Tartaglia, R. Yamada, Development and test of Nb_3Sn cos-theta dipoles based on PIT strands, IEEE Trans. Appl. Supercond. 15 (2) (2005) 1160.

[60] A. V. Zlobin, G. Ambrosio, N. Andreev, E. Barzi, B. Bordini, R. Bossert, R. Carcagno, D. R. Chichili, J. DiMarco, L. Elementi, S. Feher, V. S. Kashikhin, V. V. Kashikhin, R. Kephart, M. Lamm, P. J. Limon, I. Novitski, D. Orris, Y. Pischalnikov, P. Schlabach, R. Stanek, J. Strait, C. Sylvester, M. Tartaglia, J. C. Tompkins, D. Turrioni, G. Velev, R. Yamada, V. Yarba, R&D of Nb_3Sn accelerator magnets at Fermilab, IEEE Trans. Appl. Supercond. 15 (2) (2005) 1113.

[61] J. A. Roeterdink, J. D. Elen, W. M. P. Franken, The ECN 12 Tesla insert coil for Sultan, in: C. Marinucci, P. Weymuth (Eds.), Proc. 9th Int. Conf. on Magnet Technology, Zurich, Switzerland, Swiss Institute for Nuclear Research, 1985, p. 402.

[62] G. Ambrosio, N. Andreev, S. E. Bartlett, E. Barzi, C.-H. Denarie, D. Dietderich, A. K. Ghosh, A. P. Verweij, A. V. Zlobin, Critical current and instability threshold measurement of Nb_3Sn cables for high field accelerator magnets, IEEE Trans. Appl. Supercond. 15 (2) (2005) 1545.

[63] A. Godeke, M. C. Jewell, P. J. Lee, D. C. Larbalestier, Possible improvements in Nb_3Sn wire properties via the reduction of inhomogeneities, Presented at the 2003 Low Temperature Superconductor Workshop, Monterey CA, USA (2003).

[64] M. C. Jewell, T. J. Gerczak, D. C. Larbalestier, Putting a different "P" in PIT: phase equilibria in high-sn intermetallics, Presentation 1MB05

at the 2006 Applied Superconductivity Conference, Seattle WA, USA (2006).

[65] C. V. Renaud Jr., T. Wong, L. R. Motowidlo, ITT Nb_3Sn processing and properties, IEEE Trans. Appl. Supercond. 15 (2) (2005) 3418.

[66] C. V. Renaud Jr., T. Wong, High field Nb_3Sn superconductors fabricated by the Internal-Tin-Tube process, Adv. Cryo. Eng. (Materials) 52B (2006) 497.

[67] M. T. Naus, Optimization of Internal-Sn Nb_3Sn composites, Ph.D. thesis, Univ. of Wisconsin-Madison (2002).

[68] L. D. Cooley, Y. F. Hu, A. R. Moodenbaugh, Enhancement of the upper critical field of Nb_3Sn utilizing disorder introduced by ball milling the elements, Appl. Phys. Lett. 88 (2006) 142506.

[69] S. Bose, P. Raychaudhuri, R. Banerjee, P. Ayyub, Upper critical field in nanostructured Nb: Competing effects of the reduction in density of states and the mean free path, Phys. Rev. B 74 (2006) 224502.